# Derivatives of the Triazoloquinazoline Adenosine Antagonist (CGS 15943) Having High Potency at the Human $A_{2B}$ and $A_3$ Receptor Subtypes

Yong-Chul Kim, Maarten de Zwart,[†] Louis Chang, Stefano Moro, Jacobien K. von Frijtag Drabbe Künzel,[†] Neli Melman, Ad P. IJzerman,[†] and Kenneth A. Jacobson*

*Molecular Recognition Section, Laboratory of Bioorganic Chemistry, National Institute of Diabetes, Digestive and Kidney Diseases, National Institutes of Health, Bethesda, Maryland 20892-0810, and Division of Medicinal Chemistry, Leiden/Amsterdam Center for Drug Research, P.O. Box 9502, 2300 RA Leiden, The Netherlands*

*Received February 11, 1998*

The adenosine antagonist 9-chloro-2-(2-furanyl)[1,2,4]triazolo[1,5-*c*]quinazolin-5-amine (CGS 15943) binds nonselectively to human $A_1$, $A_{2A}$, and $A_3$ receptors with high affinity. Acylated derivatives and one alkyl derivative of the 5-amino group and other modifications were prepared in an effort to enhance $A_{2B}$ or $A_3$ subtype potency. In general, distal modifications of the $N^5$-substituent were highly modulatory to potency and selectivity at adenosine receptors, as determined in radioligand binding assays at rat brain $A_1$ and $A_{2A}$ receptors and at recombinant human $A_3$ receptors. In Chinese hamster ovary cells stably transfected with human $A_{2B}$ receptor cDNA, inhibition of agonist-induced cyclic AMP production was measured. An $N^5$-(2-iodophenyl)acetyl derivative was highly selective for $A_{2A}$ receptors. An (*R*)-$N^5$-α-methyl-(phenylacetyl) derivative was the most potent derivative at $A_3$ receptors, with a $K_i$ value of 0.36 nM. A bulky $N^5$-diphenylacetyl derivative, **13**, displayed a $K_i$ value of 0.59 nM at human $A_3$ receptors and was moderately selective for that subtype. Thus, a large, nondiscriminating hydrophobic region occurs in the $A_3$ receptor in proximity to the $N^5$-substituent. A series of straight-chain $N^5$-aminoalkylacyl derivatives demonstrated that for $A_{2B}$ receptors the optimal chain length occurs with three methylene groups, i.e., the $N^5$-γ-aminobutyryl derivative **27** which had a p$A_2$ value of 8.0 but was not selective for $A_{2B}$ receptors. At $A_1$, $A_{2A}$, and $A_3$ receptors however the optimum occurs with four methylene groups. An $N^5$-pivaloyl derivative, which was less potent than **27** at $A_1$, $A_{2A}$, and $A_3$ receptors, retained moderate potency at $A_{2B}$ receptors. A molecular model of the **27**−$A_{2B}$ receptor complex based on the structure of rhodopsin utilizing a "cross-docking" procedure was developed in order to visualize the environment of the ligand binding site.

## Introduction

Of the four known subtypes of adenosine receptors, $A_1$, $A_{2A}$, $A_{2B}$, and $A_3$ receptors, ligand development at the first two subtypes has been well-explored for both selective agonists and antagonists.[1−3] Radioligands selective for $A_1$ receptors have been known since the early 1980s,[4] and radioligands selective for $A_{2A}$ receptors were first introduced in the late 1980s.[5] These tools have aided greatly in the identification of numerous ligands for the $A_1$ and $A_{2A}$ adenosine receptor subtypes. Such selective agonists and antagonists are potentially useful in the treatment of disorders of the CNS[6−8] and the renal system[9] and also cardiovascular disorders.[10]

Several classes of agonists and antagonists selective for the most recently cloned adenosine receptor, the $A_3$ subtype, have also been reported.[11] These agents have been used pharmacologically to demonstrate both cerebroprotective[12] (chronic agonist or acute antagonist) and cardioprotective[13] (agonist) effects. $A_3$ receptor agonists at high concentration may also induce apoptosis.[14] Four diverse chemical classes have been identified as promising leads for $A_3$ antagonists: flavonoids[15] (phenolics found in all vascular plants), pyridines,[16] dihydropyridines[17−19] (structurally similar to $Ca^{2+}$ channel antagonists), and triazoloquinazolines,[20] such as **1a** (9-chloro-2-(2-furyl)[1,2,4]triazolo[1,5-*c*]quinazolin-5-amine, CGS 15943; Chart 1). Chemical optimization of the leads has resulted in antagonists having subnanomolar affinity, for example, 5-(phenylacetylamino)-9-chloro-2-(2-furyl)[1,2,4]triazolo[1,5-*c*]quinazoline (MRS 1220, **1b**), which had a $K_i$ value in binding of 0.65 nM at human $A_3$ receptors. 1,4-Dihydropyridine derivatives **2** in some cases displayed >30000-fold selectivity for human $A_3$ receptors (e.g., MRS 1334, **2b**). Antagonist radioligands for the $A_3$ receptor are still lacking.

The adenosine $A_{2B}$ receptor[21] is the poorest characterized subtype of adenosine receptors. Whereas for the other subtypes selective agonists, antagonists, and radiolabeled ligands are available, no such compounds are known for the $A_{2B}$ receptor. For pharmacological studies, both selective agonists and antagonists are needed. An $A_{2B}$ selective antagonist may prove useful in the treatment of asthma.[43]

As an approach to find both selective antagonists for the $A_{2B}$ receptor and more potent antagonists for the $A_3$ receptor, we have synthesized and screened a series of triazoloquinazolines derived from the nonselective $A_1$/$A_{2A}$ receptor antagonist **1a**. In this study we have further explored the pharmacophore region in the vicinity of the $N^5$ position of **1a** and the acyl group of **1b** in binding to the human $A_3$ receptor and have

* Address correspondence to: Dr. K. A. Jacobson, Bldg 8A, Rm B1A-19, NIH, NIDDK, LBC, Bethesda, MD 20892-0810. Tel: (301) 496-9024. Fax: (301) 480-8422. E-mail: kajacobs@helix.nih.gov.

[†] Leiden/Amsterdam Center for Drug Research.

S0022-2623(98)00094-6 CCC: $15.00 
Published on Web 06/18/1998

**Chart 1.** Structures of High-Affinity $A_3$ Receptor Antagonists ($K_i$ Values in $\mu$M).

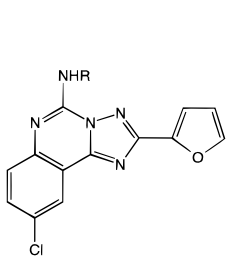

**1a**, R = H, CGS 15943

rat $A_1$ : 0.021 ± 0.003
rat $A_{2A}$ : 0.0033 ± 0.0017
human $A_3$ : 0.0138 ± 0.0024

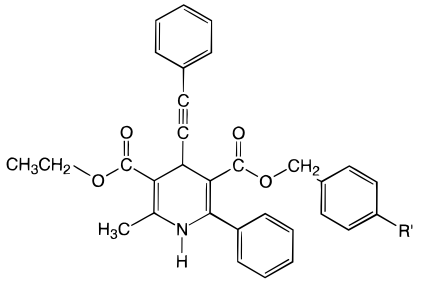

**1b**, R = $PhCH_2CO$, MRS 1220

rat $A_1$ : 0.305 ± 0.051
rat $A_{2A}$ : 0.052 ± 0.009
human $A_3$ : 0.00065 ± 0.00025

**2a**, R' = H, MRS 1191

rat $A_1$ : 40.1
rat $A_{2A}$ : >100
human $A_3$ : 0.0314

**2b**, R' = $NO_2$, MRS 1334

rat $A_1$ : >100
rat $A_{2A}$ : >100
human $A_3$ : 0.00269

**Table 1.** Affinities or Antagonistic Activities of Triazoloquinazoline Derivatives in Radioligand Binding Assays at $A_1$, $A_{2A}$, and $A_3$ Receptors[a–c]

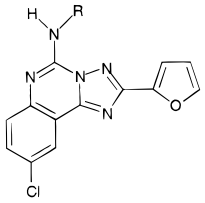

| | | $K_i$ or $IC_{50}$ (nM) | | | | |
|---|---|---|---|---|---|---|
| compd | R | $rA_1$ | $rA_{2A}$ | $hA_3$ | $rA_1/hA_3$ | $rA_{2A}/hA_3$ |
| **1a** (CGS 15943) | H | 21 ± 3.0[d] | 3.3 ± 1.7[d] | 13.8 ± 2.4 | | |
| **1b** | $COCH_2$-Ph | 52.7 ± 11.8[e] | 10.3 ± 3.7[e] | 0.65 ± 0.25 | 81 | 16 |
| **3** | $CH_2$-Ph | 1200 ± 15 | 200 ± 34 | 42.5 ± 6.91 | 28 | 4.7 |
| **4** | $COCH_2$-(4-$CH_3O$-Ph) | 30.2 ± 6.3 | 28.0 ± 4.8 | 14.4 ± 3.2 | 2.1 | 1.9 |
| **5** | $COCH_2$-(4-$NH_2$-3-I-Ph) | 217 ± 65 | 10.4 ± 2.2 | 49.3 ± 17.9 | 4.4 | 0.21 |
| **6** | $COCH_2$-(4-$NH_2$-Ph) | 24.9 ± 7.7 | 6.97 ± 1.13 | 3.56 ± 1.24 | 7.0 | 2.0 |
| **7** | $COCH_2$-(2-I-Ph) | 2300 ± 590 | 17.2 ± 4.0 | >10000 | <1 | ≪1 |
| **8** | $COCH_2$-(3-I-Ph) | 45.4 ± 8.7 | 9.67 ± 1.74 | 882 ± 242 | 0.051 | 0.011 |
| **9** | $COCH_2$-(4-I-Ph) | 13.8 ± 4.6 | 9.93 ± 2.00 | 62.9 ± 13.0 | 0.22 | 0.16 |
| **10** | $COCH_2$-(3-Cl-Ph) | 43.0 ± 6.4 | 9.43 ± 2.65 | 32.1 ± 11.3 | 1.3 | 0.29 |
| **11** | (*R*)-$COCH(CH_3)$(Ph) | 46.2 ± 11.9 | 11.1 ± 1.3 | 0.362 ± 0.053 | 130 | 31 |
| **12** | (*S*)-$COCH(CH_3)$(Ph) | 37.5 ± 8.5 | 20.1 ± 3.7 | 0.468 ± 0.111 | 80 | 43 |
| **13** | $COCH(Ph)_2$ | 129 ± 43 | 12.1 ± 3.4 | 0.586 ± 0.196 | 220 | 21 |
| **14** | $COC(CH_3)(Ph)_2$ | 890 ± 131 | 453 ± 156 | 194 ± 42 | 4.6 | 2.3 |
| **15** | $COCH_2CH_2$-Ph | 45.2 ± 7.5 | 28.3 ± 10.3 | 23.6 ± 7.6 | 1.9 | 1.6 |
| **16** | COCH=CH-Ph (*trans*) | 282 ± 71 | 59.8 ± 13.4 | 72.1 ± 15.6 | 3.9 | 0.71 |
| **17** | D-$COCH(CH_3)$(NH-Boc) | 48.6 ± 6.7 | 18.8 ± 5.3 | 46.3 ± 5.4 | 1.0 | 0.41 |
| **18** | L-$COCH(CH_3)$(NH-Boc) | 54.7 ± 13.4 | 6.65 ± 1.56 | 82.9 ± 2.7 | 0.66 | 0.080 |
| **19** | $CO(CH_2)_2$-NH-Boc | 31.0 ± 2.2 | 7.58 ± 0.80 | 6.71 ± 0.67 | 4.6 | 1.1 |
| **20** | $CO(CH_2)_3$-NH-Boc | 45.9 ± 13.2 | 19.9 ± 4.6 | 32.9 | 1.4 | 0.60 |
| **21** | $CO(CH_2)_4$-NH-Boc | 30.1 ± 6.8 | 3.64 ± 0.34 | 22.0 ± 3.1 | 1.4 | 0.17 |
| **22** | $CO(CH_2)_5$-NH-Boc | 53.8 ± 12.7 | 33.7 ± 7.3 | 33.8 ± 10.2 | 1.6 | 1.0 |
| **23** | $CO(CH_2)_6$-NH-Boc | 38.2 ± 2.6 | 11.1 ± 1.9 | 53.7 ± 31.0 | 0.71 | 0.21 |
| **24** | D-$COCH(CH_3)(NH_2)$ | 193 ± 17 | 29.7 ± 9.1 | 1140 ± 370 | 0.17 | 0.026 |
| **25** | L-$COCH(CH_3)(NH_2)$ | 390 ± 127 | 143 ± 13 | 1200 ± 460 | 0.33 | 0.12 |
| **26** | $CO(CH_2)_2$-$NH_2$ | 89.8 ± 23.3 | 7.58 ± 2.1 | 874 ± 4 | 0.10 | 0.0088 |
| **27** | $CO(CH_2)_3$-$NH_2$ | 8.75 ± 2.28 | 1.38 ± 0.23 | 80.8 ± 7.4 | 0.11 | 0.017 |
| **28** | $CO(CH_2)_4$-$NH_2$ | 6.99 ± 1.38 | 1.13 ± 0.41 | 57.9 ± 20.8 | 0.12 | 0.020 |
| **29** | $CO(CH_2)_5$-$NH_2$ | 99.6 ± 6.7 | 10.3 ± 3.7 | 213 ± 27 | 0.47 | 0.048 |
| **30** | $CO(CH_2)_6$-$NH_2$ | 114 ± 26 | 55.9 ± 5.5 | 346 ± 77 | 0.33 | 0.16 |
| **31** | $CO(CH_2)_4$-COOBn | 304 ± 126 | 16.7 ± 2.5 | 44.7 ± 14.1 | 6.8 | 0.37 |
| **32** | $CO(CH_2)_2$-$COOCH_3$ | 71.8 ± 7.2 | 28.8 ± 10.7 | 55.1 ± 8.6 | 1.3 | 0.52 |
| **33** | $CO(CH_2)_6$-$COOCH_3$ | 46.6 ± 10.5 | 7.43 ± 2.72 | 59.0 ± 18.1 | 0.79 | 0.13 |
| **34** | $CO(CH_2)_3$-COOH | 45 ± 4 | 1.15 ± 0.47 | 81.3 ± 11.0 | 0.55 | 0.014 |

[a] Displacement of specific [$^3$H]*R*-PIA binding in rat brain membranes, expressed as $K_i$ ± SEM ($n$ = 3–5). [b] Displacement of specific [$^3$H]CGS 21680 binding in rat striatal membranes, expressed as $K_i$ ± SEM ($n$ = 3–6). [c] Displacement of specific [$^{125}$I]AB-MECA binding at human $A_3$ receptors expressed in HEK cells, in membranes, expressed as $K_i$ ± SEM ($n$ = 3–4). [d] $IC_{50}$ values for **1a** (see ref 20). [e] Previously reported $K_i$ values were 305 and 52.0 nM for rat $A_1$ and $A_{2A}$ receptors, respectively.[20]

defined the previously unknown structure–activity relationship (SAR) at the human $A_{2B}$ receptor.

## Results and Discussion

**Synthesis.** The structures of the triazoloquinazoline derivatives tested for affinity in radioligand binding assays at adenosine receptors are shown in Table 1. A few derivatives, e.g., the phenylacetyl derivative **1b** and the 5-aminoacyl derivatives **20** and **27** in Table 1 and compounds **35**–**46** in Table 3, had been reported by us previously.[20] The 5-benzyl derivative **3** was prepared through an alkylation reaction using potassium hydrox-

**Table 2.** Yields and Chemical Characterization of Triazoloquinazoline Derivatives

| compd no. | % yield | mp (°C) | MS | formula | anal. |
|---|---|---|---|---|---|
| **3** | 29 | 184−185 | EI: 375 | $C_{20}H_{14}N_5O_2Cl\cdot0.81H_2O$ | C,H,N |
| **4** | 12 | 258−260 | EI: 433 | $C_{22}H_{16}N_5O_3Cl\cdot0.53CH_2Cl_2$ | C,H,N |
| **5** | 25 | 210−211 | CI: 545 | $C_{21}H_{14}N_6O_2ClI$ | C,H,N |
| **6** | 45 | 197−199 | EI: 418 | $C_{21}H_{15}N_6O_2Cl\cdot0.64H_2O$ | C,H,N |
| **7** | 22 | 280−282 | EI: 529 | $C_{21}H_{13}N_5O_2ClI\cdot0.94(CH_3)_2CO$ | C,H,N |
| **8** | 16 | 224−227 | CI: 530 | $C_{21}H_{13}N_5O_2ClI\cdot1.17(CH_3)_2CO$ | C,H,N |
| **9** | 51 | 260−262 dec | EI: 529 | $C_{21}H_{13}N_5O_2ClI$ | C,H,N |
| **10** | 33 | 248−250 | CI: 438 | $C_{21}H_{13}N_5O_2Cl_2$ | C,H,N |
| **11** | 38 | 207−209 dec | EI: 417 | $C_{22}H_{16}N_5O_2Cl$ | C,H,N |
| **12** | 58 | 115−118 | EI: 417 | $C_{22}H_{16}N_5O_2Cl$ | C,H,N |
| **13** | 57 | 205−207 | CI: 480 | $C_{27}H_{18}N_5O_2Cl$ | C,H,N |
| **14** | 100 | 175−178 | EI: 493 | $C_{28}H_{20}N_5O_2Cl$ | C,H,N |
| **15** | 65 | 253−255 | EI: 417 | $C_{22}H_{17}N_5O_2Cl$ | C,H,N |
| **16** | 43 | 305−307 | CI: 416 | $C_{22}H_{15}N_5O_2Cl$ | C,H,N |
| **17** | 13 | 131−134 | CI: 457 | $C_{21}H_{21}N_6O_4Cl$ | C,H,N |
| **18** | 15 | 220 | CI: 457 | $C_{21}H_{21}N_6O_4Cl\cdot2.6CH_3OH$ | C,H,N |
| **19** | 50 | 216−218 | CI: 457 | $C_{21}H_{21}N_6O_4Cl$ | C,H,N |
| **21** | 53 | 189−192 | CI: 485 | $C_{23}H_{25}N_6O_4Cl$ | C,H,N |
| **22** | 100 | 196−198 | CI: 499 | $C_{24}H_{27}N_6O_4Cl$ | C,H,N |
| **23** | 100 | 156−157 | EI: 512 | $C_{25}H_{29}N_6O_4Cl\cdot0.91H_2O$ | C,H,N |
| **24** | 56 | 175−176 | FAB: 357 | $C_{16}H_{13}N_6O_2Cl$ | FAB$^{+a}$ |
| **25** | 71 | 278 | FAB: 357 | $C_{16}H_{13}N_6O_2Cl$ | FAB$^{+a}$ |
| **26** | 72 | 137−139 | EI: 356 | $C_{16}H_{13}N_6O_2Cl\cdot CF_3COOH$ | C,H,N |
| **28** | 64 | 231−232 | FAB: 385 | $C_{18}H_{17}N_6O_2Cl$ | FAB$^{+a}$ |
| **29** | 80 | 153−155 | CI: 399 | $C_{19}H_{19}N_6O_2Cl\cdot CF_3COOH\cdot0.87CH_3OH$ | C,H,N |
| **30** | 70 | 165−167 | EI: 412 | $C_{20}H_{21}N_6O_2Cl$ | FAB$^{+a}$ |
| **31** | 71 | 149−151 | EI: 503 | $C_{26}H_{22}N_5O_4Cl\cdot CF_3COOH$ | C,H,N |
| **32** | 54 | 185−187 | EI: 399 | $C_{18}H_{14}N_5O_4Cl\cdot0.3EtOAc$ | C,H,N |
| **33** | 62 | 165 | EI: 455 | $C_{22}H_{22}N_5O_4Cl\cdot0.37(C_2H_5)_2O$ | C,H,N |
| **34** | 26 | 209−211 | FAB: 400 | $C_{18}H_{14}N_5O_4Cl\cdot0.56CH_2Cl_2$ | C,H,N |

[a] High-resolution mass in FAB$^+$ mode (*m*/*z*) determined to be within acceptable limits. **24**: calcd, 357.0867; found, 357.0879. **25**: calcd, 357.0867; found, 357.0865. **28**: calcd, 385.1180; found, 385.1168. **30**: calcd, 413.1491; found, 413.1493.

ide and benzyl bromide. The 4-amino-3-iodophenylacetyl derivative **5** was synthesized by iodination[22] (using iodine and calcium carbonate) of the 4-aminophenylacetyl derivative **6** which was prepared from catalytic reduction of the corresponding 4-nitrophenylacetyl derivative. The other various acyl derivatives were synthesized using standard acylation methods described in the Experimental Section, except for the 4-carboxybutanoyl congener **34** which was prepared by heating with glutaric anhydride at 80 °C without base or coupling agents. The *R*- and *S*-enantiomeric pairs (**11** and **14**; **17** and **18**) were prepared from the corresponding optically pure carboxylic acids. The yields and chemical characterization of these compounds are reported in Table 2.

**Affinity at Adenosine Receptors. Binding Assays at $A_1$, $A_{2A}$, and $A_3$ Receptors.** $K_i$ values were determined in radioligand binding assays at rat cortical $A_1$ receptors vs [$^3$H]*R*-PIA ([$^3$H]-(*R*)-$N^6$-(phenylisopropyl)adenosine) and at rat striatal $A_{2A}$ receptors vs [$^3$H]CGS 21680 ([$^3$H]-2-[[4-(2-carboxyethyl)phenyl]ethylamino]-5′-(*N*-ethylcarbamoyl)adenosine).[4,5] Affinity at cloned human $A_3$ receptors expressed in HEK-293 cells[23] was determined using [$^{125}$I]AB-MECA ($N^6$-(4-amino-3-[$^{125}$I]iodobenzyl)-5′-(*N*-methylcarbamoyl)adenosine).[24]

$N^5$-Alkylation in the *N*-benzyl derivative **3** decreased binding affinity at $A_1$, $A_{2A}$, and $A_3$ receptors. Simple phenyl ring substitutions were made on the structure of the $N^5$-phenylacetyl derivative **1b** including: methoxy, **4**; amino, **5** and **6**; and halo, **7**−**10**. None of these derivatives exceeded the affinity of **1b** at human $A_3$ receptors. The most potent of these derivatives was the 4-amino derivative **6** which was prepared as a potential substrate for radioiodination. The $K_i$ value of **6** at human $A_3$ receptors was 3.56 nM, which would have been satisfactory for a radioligand; however upon iodination to give compound **5**, the affinity at human $A_3$ receptors decreased by 14-fold. Thus, the receptor affinity is highly dependent on the substitution of the phenyl ring of **1b**. The affinities of ring-iodinated isomers of **1b**, **7**−**9**, were compared. The $N^5$-(2-iodophenyl)acetyl derivative **7** was highly selective for $A_{2A}$ receptors. The $N^5$-(3-chlorophenyl)acetyl and $N^5$-(3-iodophenyl)acetyl derivatives **10** and **8**, respectively, differed in affinity only at the $A_3$ receptor, such that **8** was 27-fold less potent in binding.

Substitution of the two prochiral methylene hydrogens of the acetyl group was carried out. The α-methyl substitutions, resulting in the *R*- and *S*-enantiomers **11** and **12**, appeared to slightly enhance affinity in both cases. No significant stereoselectivity of binding to $A_1$, $A_{2A}$, and $A_3$ receptors was evident at this chiral center. The most potent derivative at $A_3$ receptors in the present study was the (*R*)-$N^5$-α-methyl(phenylacetyl) derivative **11** with a $K_i$ value of 0.36 nM. Curiously, even a phenyl substitution at the methylene group, compound **13**, resulted in extremely high affinity at human $A_3$ receptors, with a $K_i$ value of 0.59 nM and selectivities of 220- and 21-fold vs rat $A_1$ and $A_{2A}$ receptors, respectively. Thus, the binding region of the receptor surrounding the α-carbon of the acetyl group of **1b** is not highly sterically restricted. Nevertheless, retention of at least one methylene hydrogen of the acetyl group was required for high affinity at the adenosine receptors, since the α-methyldiphenyl derivative **14** was 330-fold less potent than the α-diphenyl derivative **13** in binding to human $A_3$ receptors. Homologation of **1b** to give the phenylpropionyl derivative **15** reduced the affinity at human $A_3$ receptors by 27-

**Table 3.** Potency of Triazoloquinazoline Derivatives in a Functional Assay at Human $A_{2B}$ Receptors Stably Expressed in CHO Cells

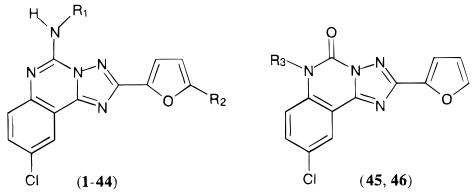


$R_2$ = H, unless noted

| compd | $R_1$ or $R_3$ | % inhibition[a,c] | $IC_{50}$ ($\mu$M)[b,d] | p$A_2$[d] |
|---|---|---|---|---|
| **1a** | H | 100 (100−100) | 1.20 ± 0.43 | 8.0 ± 0.3 |
| **1b** | $COCH_2$-Ph | 71 (73−69) | | |
| **3** | $CH_2$-Ph | 21 (20−22) | | |
| **5** | $COCH_2$(4-$NH_2$-3-I-Ph) | 23 (18−27) | | |
| **6** | $COCH_2$(4-$NH_2$-Ph) | 90 (85−94) | 7.4 ± 4.5 | |
| **9** | $COCH_2$-(4-I-Ph) | 42 (39−45) | | |
| **10** | $COCH_2$-(3-Cl-Ph) | 45 (55−34) | | |
| **15** | $COCH_2CH_2$-Ph | 43 (50−36) | | |
| **16** | COCH=CH-Ph | 38 ± 14 | | |
| **20** | $CO(CH_2)_3$-NH-Boc | 47 (57−36) | | |
| **26** | $CO(CH_2)_2$-$NH_2$ | 83 (85−80) | 13.3 ± 4.0 | |
| **27** | $CO(CH_2)_3$-$NH_2$ | 100 (100−100) | 0.27 ± 0.04 | 8.0 ± 0.3 |
| **28** | $CO(CH_2)_4$-$NH_2$ | 100 (100−100) | 1.77 ± 1.25 | |
| **29** | $CO(CH_2)_5$-$NH_2$ | 79 (73−85) | | |
| **30** | $CO(CH_2)_6$-$NH_2$ | 75 (74−75) | | |
| **34** | $CO(CH_2)_3$-COOH | | 1.90 ± 0.13 | |
| **35** | $COCH_3$ | 92 (94−90) | 2.65 ± 1.00 | |
| **36** | $COCH_2CH_3$ | 66 (75−56) | | |
| **37** | $CO(CH_2)_2CH_3$ | 66 (73−58) | | |
| **38** | $CO(CH_2)_3CH_3$ | 79 (86−72) | | |
| **39** | $COC(CH_3)_3$ | 89 (92−85) | 2.40 ± 1.70 | |
| **40** | CO-$OC(CH_3)_3$ | 92 (94−90) | 2.41 ± 1.02 | |
| **41** | CO-Ph | 58 (69−47) | | |
| **42** | CO-(3-I-Ph) | 38 (51−25) | | |
| **43** | H, $R_2$ = Br | 16 (24−9) | | |
| **44** | CO-Ph, $R_2$ = Br | 0 (0−0) | | |
| **45** | H | 0 (0−0) | | |
| **46** | $(CH_2)_2CH_3$ | 0 (0−0) | | |

[a] Percentage inhibition by 50 $\mu$M of each antagonist of cyclic AMP production induced by 50 $\mu$M NECA. [b] Concentration of antagonist inhibiting 50% of cyclic AMP production induced by 50 $\mu$M NECA. [c] Values are the means of duplicate measurements (values of individual measurements between parentheses) or are the means of at least three experiments ± SEM. [d] Values are given ± SEM and are the means of at least three experiments.

fold, and the corresponding styryl derivative **16** was even less potent at $A_3$ receptors.

The $\gamma$-aminobutyric acid derivatives, both the Boc-protected form **20** and the free amino form **27**, were reported in the previous study.[20] The SAR of homologues of these derivatives was explored. Although nanomolar affinities at human $A_3$ receptors were not obtained, there was a distinct dependence of affinity upon lengthening or shortening the methylene chain. A minimum in the $K_i$ values at $A_1$, $A_{2A}$, and $A_3$ receptors among the free amine derivatives was obtained at a chain length of four methylene groups, corresponding to compound **28** (Figure 1), which had a $K_i$ value of 1.13 nM at $A_{2A}$ receptors. For free amine derivatives, the order of affinity was invariably: $A_{2A} > A_1 > A_3$ receptors. Thus, the interactions responsible for this affinity enhancement must be common to these three receptor subtypes. For Boc-amine derivatives, however, a clear dependence of binding affinity on chain length was not evident at $A_1$, $A_{2A}$, and $A_3$ adenosine receptor subtypes. In this series of amino acid derivatives, no stereoselectivity of binding to $A_1$, $A_{2A}$, and $A_3$ receptors was evident at the α-carbon prochiral center, as seen from the affinities of the D- and L-Ala conjugates, **17** vs **18** and **24** vs **25**. At $A_{2A}$ receptors the presence of the free amino group, e.g., **27**−**29**, in general resulted in higher affinity, while at $A_3$ receptors the Boc-protected form, e.g., **20**−**22**, appeared to be preferred. This suggested that human $A_3$ receptors contain a more highly hydrophobic pocket in this region than do rat $A_{2A}$ receptors. Furthermore, at $A_1$ receptors the free amine is preferred over the Boc-amine for analogues containing three and four methylene groups.

The effects of ester, **31**−**33**, and carboxylic acid, **34**, groups on the $N^5$-acyl substituent were also explored. The affinity at $A_3$ receptors was not significantly affected by the presence of a negatively charged carboxylate group vs a neutral ester group.

**Functional Assay at $A_{2B}$ Receptors.** Compound **1a** and selected $N^5$-acyl-substituted analogues (Table 3) were screened by measuring the percentage inhibition by the analogue (50 $\mu$M) of the cyclic AMP production induced by 50 $\mu$M 5′-(*N*-ethylcarboxamido)adenosine (NECA) in a Chinese hamster ovary cell line stably transfected with human $A_{2B}$ receptor cDNA. For derivatives that displayed ≥80% inhibition, $IC_{50}$ values were determined on cyclic AMP production induced by 50 $\mu$M NECA. Finally, p$A_2$ values were determined for two of the most active derivatives, **1a** and **27**. For this purpose, NECA concentration−response curves were recorded in the absence and presence of three increasing concentrations of antagonist. p$A_2$ values were derived from Schild plots (Figure 1), which displayed slopes of approximately unity.

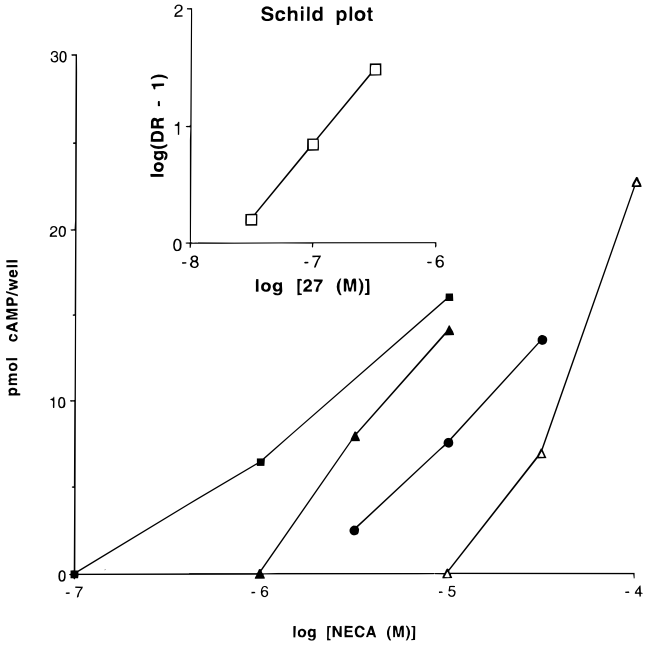


**Figure 1.** Determination of the p$A_2$ value of compound **27** at human $A_{2B}$ receptors. Data were taken from a typical experiment. Dose−response curves of NECA were recorded in the absence and presence of three concentrations of the antagonist **27**: ■, no antagonist added; ▲, 0.03 $\mu$M; ●, 0.1 $\mu$M; Δ, 0.3 $\mu$M. p$A_2$ values were determined in a Schild plot (inset) with a slope of approximately unity.

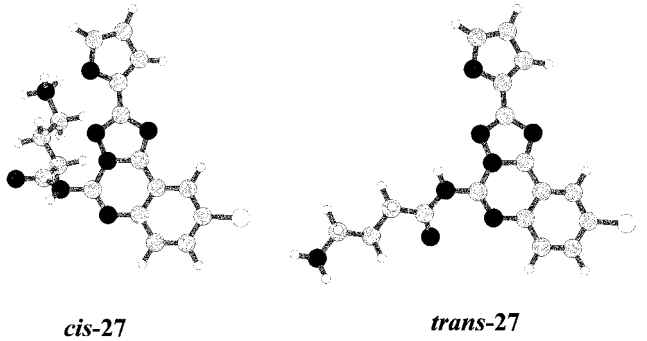


**Figure 2.** Minimized energy conformations of **27**, showing two conformers (cis and trans) of the aminoalkyl side chain.

Compound **1a** had an $IC_{50}$ value of 1.20 $\mu$M. In the same system a p$A_2$ value of 8.0 ± 0.3 was measured. This agrees with earlier findings of Alexander et al., who have measured a value of 7.8 in a similar assay, using another CHO cell line expressing human $A_{2B}$ receptors.[42] The $\gamma$-aminobutyryl-substituted derivative **27** displayed an elevated potency at the $A_{2B}$ receptor ($IC_{50}$ value of 0.27 $\mu$M). However, its p$A_2$ value was similar to that of **1a**. Concentration−response curves of NECA in the presence and absence of **27** are shown in Figure 2. There was no gain in selectivity toward the other receptor subtypes.

Derivatives with a 2-(5-bromofuryl) substituent (**43**, **44**) and derivatives that lack the 5-amino function (**45**, **46**) were weak or inactive as $A_{2B}$ receptor antagonists. Diminished affinities of these analogues for the other subtypes have been reported previously.[20]

Among the amino acid conjugates a minimum in the $IC_{50}$ values in $A_{2B}$ receptor antagonism was observed with a chain length of three methylene groups (**27**), while at $A_1$, $A_{2A}$, and $A_3$ receptors aminoalkyl derivatives having three and four methylene groups were nearly equipotent. At $A_{2B}$ receptors the Boc-protected $\gamma$-aminobutyryl derivative **20** had a much lower activity than the corresponding free amino derivative **27** (only 47% inhibition at 50 $\mu$M).

The $\gamma$-carboxybutyryl derivative **34** showed a high potency (1.9 $\mu$M), but it was less active than the $\gamma$-aminobutyryl derivative **27**. Apparently, a positively charged amino group results in a higher activity than a negatively charged carboxylate function.

In the $N^5$-phenylacetyl-substituted series only the 4-amino derivative **6** displayed a moderate potency (7.4 $\mu$M). A phenylacetyl group appears to be not well-tolerated in the $A_{2B}$ receptor. Increase of potency by substitution with an amino function was also observed in propionyl, **36**, vs 3-aminopropionyl, **26**, and butyryl, **37**, vs 4-aminobutyryl, **27**, not only at the $A_{2B}$ receptor (Table 3) but also at $A_1$ and $A_{2A}$ receptors (refer to binding data of **36** and **37** in ref 20).

In the series of compounds with $N^5$-acyl chain substituents, the $N^5$-acetyl (**35**) and $N^5$-pivaloyl (**39**) derivatives were most active. Apparently, there is room in the $A_{2B}$ receptor for a bulky *tert*-butyl group. The $N^5$-Boc-substituted derivative **40**, with a *tert*-butyl group too, showed a similar activity. Remarkably, for maximal activity, the $N^5$-acetyl group should either be unsubstituted as in **35** or methyl-trisubstituted as in **39**, but not methyl-monosubstituted as in the propionyl derivative **36**.

Although the $N^5$-pivaloyl derivative **39** had a slightly decreased activity ($IC_{50}$ value 2.4 $\mu$M), it showed largely diminished affinities for $A_1$, $A_{2A}$, and $A_3$ receptors in the previous study ($K_i$ $A_1$ = 205 ± 20 nM; $K_i$ $A_{2A}$ = 88.8 ± 20.5 nM; $K_i$ $A_3$ = 244 ± 6 nM).[20] The $N^5$-Boc-substituted derivative **40** with an $IC_{50}$ value of 2.41 ± 1.02 $\mu$M behaved similarly ($K_i$ $A_1$ = 190 ± 16 nM; $K_i$ $A_{2A}$ = 92 ± 8 nM; $K_i$ $A_3$ = 82.5 ± 23.3 nM).[20] Thus, $N^5$-pivaloyl or $N^5$-Boc substitution might lead to $A_{2B}$ receptor selectivity.

**Molecular Modeling.** A rhodopsin-based molecular model for the human $A_{2A}$ receptor has been published previously.[25] As an aid in interpreting the present results at the human $A_{2B}$ receptor, we provide the first description of ligand−$A_{2B}$ receptor interactions, using **27** as a ligand to probe the $A_{2B}$ receptor binding pocket. We have recently introduced the *cross-docking* procedure[26] (see the Experimental Section) which can be considered a further refinement in building the putative antagonist binding site in the human $A_{2B}$ receptor. As with other G protein-coupled receptor models,[27] the length of the transmembrane region is approximately 40 Å. The interhelical distance between pairs of adjacent helical axes is roughly 10 Å, consistent with a common interhelical contact distance.[28] The interhelical angles, measured between the principal axes of adjacent helices, are around −150−170° for antiparallel and 10−25° for the parallel helices. This is typical of a 3−4 type helix−helix contact associated with optimal interactions between nearly parallel-aligned helices.[28] Each helix maintained almost the same position and tilting found in the published rhodopsin 2D electron density map.[29,30]

In all our calculations, we used the $\gamma$-amino-protonated form of compound **27**, consistent with protonation at physiological pH. Since **27** has high conformational

flexibility in the region of the γ-aminobutyryl side chain, a complete random search conformational analysis was performed. After sampling and minimization procedures, two energetically important conformers have been selected, one of these with the amide bond in the cis conformation and the other one in which the amide bond was in the trans conformation (see Figure 2). RHF/AM1 semiempirical calculations were conducted to obtain the optimized geometries. Only the cis conformer may be docked in an energetically favorable manner inside the TM bundle. The trans isomer would force the aminobutyl side chain toward the transmembrane helices leading to an overall distortion of the receptor architecture.

Moreover, in the cross-docked model TM3, TM4, TM5, TM6, and TM7 were rotated clockwise by 15°, 10°, 5°, 10°, and 5°, respectively, about their transmembrane axes with respect to the ligand−free receptor model. The energy of the **27**−$A_{2B}$ receptor complex structure was lowered 55 kcal/mol through the *cross-docking* procedure. Consistent with the proposal of Gouldson et al.,[31] rotations and translations of the TM domains are crucial factors in the ligand recognition process in different GPCRs. Consequently, our approach to docking is designed to mimic the natural domain movement within a receptor.

One of the most important limitations in the correct identification of the ligand binding regions of the $A_{2B}$ receptor is that no site-directed mutagenesis studies are available. Using both the $A_{2A}/A_{2B}$ sequence homology and the site-directed mutagenesis results previously obtained in our laboratory for the human $A_{2A}$ receptor,[25] we were able to identify a hypothetical binding site for **27** in the human $A_{2B}$ receptor. Figure 3 shows the 3D structural models of the human $A_{2B}$ receptor after the application of *cross-docking* with **27**.

We identified the hypothetical binding site of **27** in proximity to TMs 3, 5, 6, and 7, with the furan ring pointing toward the extracellular environment. The γ-aminobutyryl side chain is located midway between His251 (TM6) and His280 (TM7). According to the previously reported site-directed mutagenesis results for $A_1$ and $A_{2A}$ receptors,[32,25] these two histidine residues (conserved in the same positions of TM6 and TM7 helices for both receptors) were found crucial for the binding of both agonists and antagonists.

The oxygen atom of Ser283 (TM7) is within hydrogen-bonding distance (2.6 Å) of the carbonyl group of the amide moiety at the 5-position of the triazoloquinazoline structure. The amide group is surrounded by four polar amino acids: His251 (TM6), Ser279 (TM7), His280, and Ser283 (TM7). This region seems to be very important for the recognition of the antagonist structures. In particular, our side-directed mutagenesis results for human $A_{2A}$ receptor suggested that this serine (Ser281) was crucial for binding of both agonists and antagonists.[25]

Another important interaction (1.9 Å) is possible between the amino group of Asn254 (TM6) and the protonated nitrogen of the γ-aminobutyryl side chain. Also this Asn, conserved among all adenosine receptor subtypes, was found important for ligand binding. This interaction can explain the common trend observed between the different adenosine receptor subtypes, of the affinity values upon lengthening or shortening of the methylene chain. A minimum in the $K_i$ values at $A_1$, $A_{2A}$, $A_{2B}$, and $A_3$ among the free amine derivatives was obtained at chain lengths of three or four methylene groups, indicating that there is a common anchor point inside the receptor binding cavity. We speculate that Asn254 (TM6) corresponds to this anchor point in the human $A_{2B}$ receptor.

A hydrophobic region, delimited by three apolar amino acids such as Val85 (TM3), Phe187 (TM5), and Val191 (TM5), is also present in the binding site model. The corresponding amino acids Leu90 (TM3) and Phe182 (TM5) were essential for binding of both agonists and antagonists at human $A_{2A}$ receptors.[25] The chlorophenyl moiety of the triazoloquinazoline structure of **27** is located within this region. No direct interactions are predicted between the two polar amino acids, Thr89 (TM3) and Ser92 (TM3), and the antagonist structure. As previously reported, these two amino acids are important only for the coordination of the agonist derivatives at $A_1$ and $A_{2A}$ receptors, respectively.[25]

Another unresolved question is why there are great differences in ligand affinities between $A_{2A}$ and $A_{2B}$ receptors. A comparison of the nature of the critical amino acids in the TM regions involved in the recognition of the ligand at the $A_{2A}$ and $A_{2B}$ subtypes fails to provide a clear explanation. In fact, there is a very good correspondence between the important residues found using site-directed mutagenesis of the human $A_{2A}$ receptor and those present in the $A_{2B}$ receptor. We speculate that there are two important differences between the molecular structures of $A_{2A}$ and $A_{2B}$ receptors: (i) the replacement of two amino acids, Leu267 ($hA_{2A}$) with Lys269 ($hA_{2B}$) and Tyr270 ($hA_{2A}$) with Asn273 ($hA_{2B}$), at the top of TM7 that could be involved in the movement of the ligand into the binding site and (ii) the different primary and secondary structures of the second extracellular loops that seem to be involved in the extracellular recognition process of the ligand.[33] The second extracellular loop has been shown to be important for both agonist and antagonist binding at the human $A_{2A}$ receptor and could represent one of the strategic keys of the different selectivities between the different receptor subtypes.

## Experimental Section

**Computational Methods.** The human $A_{2B}$ receptor model was built and optimized using SYBYL 6.3[34] and MacroModel 5.0[35] modeling packages, respectively, based on the approaches described by van Rhee et al.[36] and Moro et al.[26] All calculations were performed on a Silicon Graphics Indigo2 R8000 workstation. Briefly, transmembrane domains were identified with the aid of Kyte−Doolittle hydrophobicity[37] and $E_{mini}$[37] surface probability parameters. Transmembrane helices were built from the sequences and minimized individually. The minimized helices were then grouped together to form a helical bundle matching the overall characteristics of the electron density map of rhodopsin. The helical bundle was minimized using the Amber[38] all-atom force field, until the rms value of the conjugate gradient (CG) was <0.1 kcal/mol/Å. A fixed dielectric constant = 4.0 was used throughout these calculations.

A model of 5-[(6-aminohexanoyl)amino]-9-chloro-2-(2-furanyl)-[1,2,4]triazolo[1,5-*c*]quinazoline (**27**) was constructed using the Sketch Molecule module of SYBYL. Conformational analysis of **27** was performed on all rotatable bonds of the aminohexanoyl side chain, using the random search procedure of

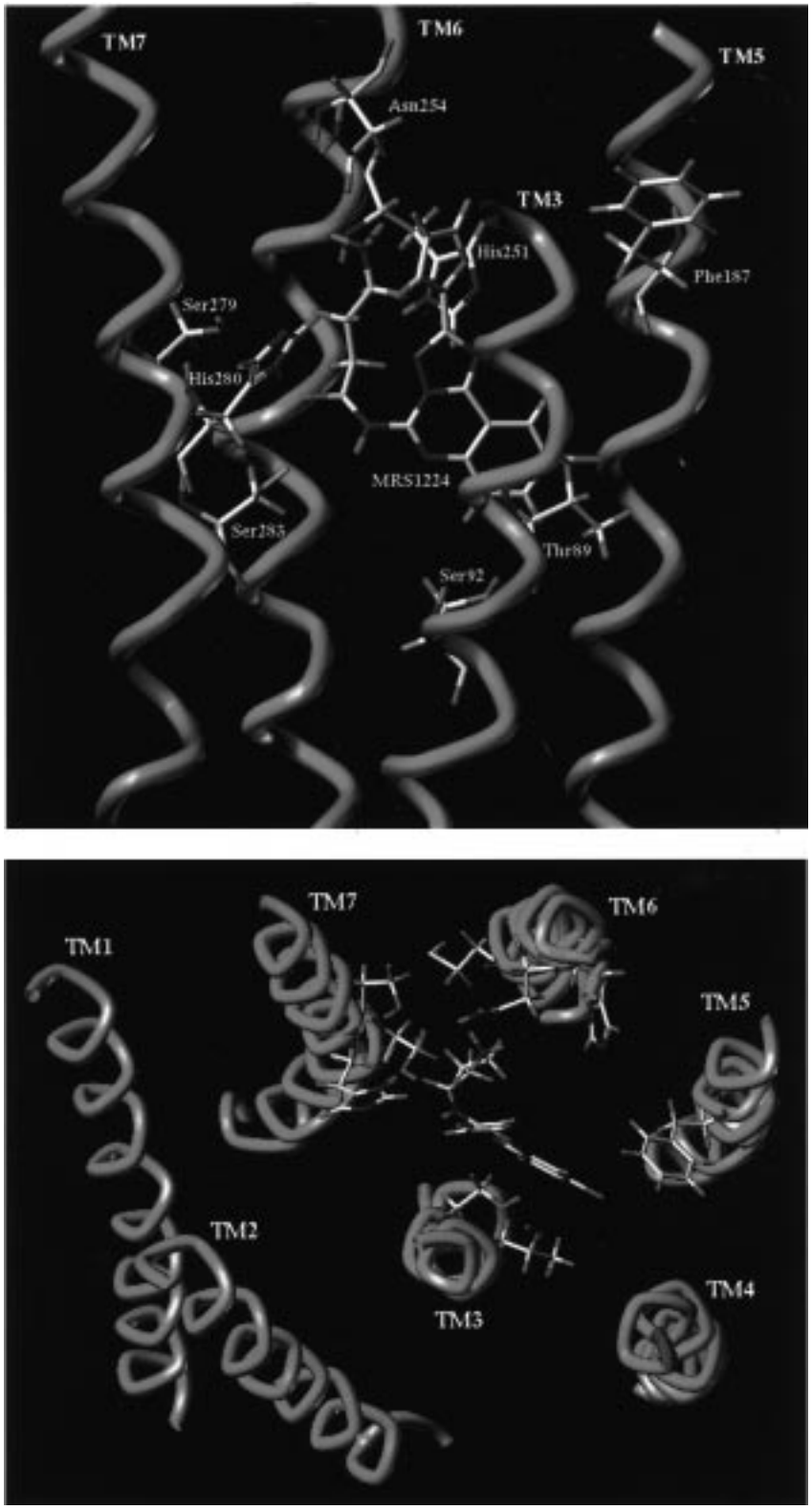


**Figure 3.** Model of the cis conformation of **27** docked in the putative binding site of the human $A_{2B}$ receptor, as viewed from the plane of the plasma membrane (top) and from the extracellular side (bottom).

SYBYL. The optimized geometries of the resulting conformers were calculated using MOPAC software (RHF method and AM1 Hamiltonian, keywords: PREC, GNORM=0.1, EF).

The fully minimized conformers were rigidly docked into the helical bundle using graphical manipulation coupled to continuous energy monitoring (Dock module of SYBYL). When a final position was reached, consistent with a local energy minimum, the complexes of receptor and ligand were subjected to an additional CG minimization run of 300 steps. Partial atomic charges for the ligands were imported from the MOPAC output files.

Recently, we have introduced a "*cross-docking*" procedure to obtain energetically refined structures of ligand−$P2Y_1$ receptor complexes.[26] We applied the same technique to obtain the structure of the **27**−$A_{2B}$ receptor complex. This is a way to explore possible ligand-induced rearrangements of 7TM

bundle by sampling 7TM conformations in the presence of the docked ligands. *Cross-docking* was carried out using the Dock module of SYBYL. Each helix was separated from the ligand−receptor complex structure, and its relative position was changed until a new lower-energy geometry was obtained. These adjustments consisted of small translations and rotations of the principal axis of the helix with respect to its original position. When a new final position was reached, consistent with the lowest-local-energy minimum, the separated helix was merged again into the ligand−receptor complex. The hydropathy profile for the new oriented helix was checked using the Kyte−Doolittle method.[37] The new complex was subjected to an additional CG minimization run of 300 steps. This procedure was repeated for TM3, TM4, TM5, TM6, and TM7. The manual adjustments were followed by 25 ps of molecular dynamics (MD module of MacroModel) performed at a constant temperature of 300 K using a time step of 0.001 ps and a dielectric constant = 4.0. This procedure was followed by another sequence of CG energy minimization to a gradient threshold of < 0.1 kcal/mol/Å. Energy minimization of the complex was performed using the AMBER all-atom (MacroModel) force field.

**Materials.** Compound **1a**, *R*-PIA, and 2-chloroadenosine were purchased from Research Biochemicals International (Natick, MA). All acylating agents were obtained from Aldrich (St. Louis, MO).

**Synthesis.** Proton nuclear magnetic resonance spectroscopy was performed on a Varian GEMINI-300 spectrometer, and spectra were taken in DMSO-$d_6$ or $CDCl_3$. Unless noted, chemical shifts are expressed as ppm downfield from tetramethylsilane. Chemical-ionization (CI) mass spectrometry was performed with a Finnigan 4600 mass spectrometer and electron-impact (EI) mass spectrometry with a VG7070F mass spectrometer at 6 kV. High-resolution FAB (fast atom bombardment) mass spectrometry was performed with a JEOL SX102 spectrometer using 6-kV Xe atoms. The compounds were previously desorbed from glycerol or magic bullet matrix. Optical rotation was measured using a Perkin-Elmer polarimeter 341. Elemental analysis (±0.4% acceptable) was performed by Atlantic Microlab Inc. (Norcross, GA) or Galbraith Laboratories, Inc. (Knoxville, TN). All melting points were determined with a Unimelt capillary melting point apparatus (Arthur H. Thomas Co., PA) and were uncorrected. All triazoloquinazoline derivatives showed one spot on TLC (MK6F silica, 0.25 mm, glass-backed; Whatman Inc., Clifton, NJ). Where needed, evaluation of purity was done on a Hewlett-Packard 1090 HPLC system using an OD-5-60 C18 analytical column (150 mm × 4.6 mm; Separation Methods Technologies, Inc., Newark, DE) in two different linear gradient solvent systems. One solvent system (A) was 0.1 M TEAA (pH = 5.0)/$CH_3CN$, 50:50 to 10:90, in 20 min with flow rate 1 mL/min. The other (B) was $H_2O$/MeOH, 40:60 to 10:90, in 20 min with flow rate 1 mL/min. Peaks were detected by UV absorption using a diode array detector.

**General Procedure for the Preparation of 5-*N*-Acyl Derivatives of 1a. Method A (Acid Chloride).** To a stirred solution of **1a** (20 mg, 0.07 mmol) and anhydrous pyridine (80 μL, 1.0 mmol) in 2 mL of anhydrous $CH_2Cl_2$ was added the desired acyl chloride (0.21 mmol), prepared from the acid and excess thionyl chloride (unless commercially available). The mixture was stirred at room temperature for 24 h and then evaporated to dryness under reduced pressure. The residue was purified by preparative silica gel TLC ($CH_2Cl_2$−MeOH, 50:1−75:1, or Hex:$CHCl_3$:MeOH, 1:1:0.1) to afford the desired compounds (**4**, **7**−**16**, **32**, **33**).

**Method B (Carbodiimide).** A solution of **1a** (20 mg, 0.07 mmol), the desired carboxylic acid compound (0.42 mmol), EDAC (82 mg, 0.42 mmol), DMAP (4 mg, 0.032 mmol), and triethylamine (0.146 mL, 1.05 mmol) in 3 mL of anhydrous DMF/$CH_2Cl_2$ (1:1 v/v) was stirred at room temperature for 48 h. The mixture was treated with the same procedure as method A for purification of the desired compounds (**17**−**23**, **31**).

**Method C (Deprotection of Boc Group).** To a solution of 0.02 mmol of Boc-protected amino acyl derivatives of **1a** in 1 mL of $CH_2Cl_2$ was added 50 μL of TFA, and the mixture stirred at room temperature for 10 min. The mixture was evaporated under reduced pressure, and white solids were obtained from ether or $CH_2Cl_2$/MeOH as TFA salts (**24**−**30**).

**9-Chloro-2-(2-furanyl)-5-(benzylamino)[1,2,4]triazolo-[1,5-*c*]quinazoline (3).** To a solution of **1a** (24.0 mg, 0.08 mmol) in 2 mL of anhydrous DMSO was added powdered potassium hydroxide (67.2 mg, 1.20 mmol) followed by benzyl bromide (28.8 mg, 0.17 mmol). The mixture was stirred at room temperature overnight and then diluted with 2 mL of water. The reaction product was extracted with $CHCl_3$ (10 mL × 3). The fractions were combined, neutralized with 1 N HCl, washed with water (25 mL × 2), and dried over sodium sulfate. The product was isolated from preparative silica gel TLC (hexanes−ethyl acetate, 4:1) (29%): $^1$H NMR ($CDCl_3$) $\delta$ 4.92 (2H, d, $J$ = 5.86 Hz, $-CH_2$), 6.55 (1H, t, $J$ = 5.86 Hz, NH), 6.61 (1H, t, $J$ = 1.95 Hz, H-4′), 7.28 (1H, s, H-3′), 7.36−7.49 (4H, m, aromatic-H), 7.61−7.64 (2H, m, H-8 and H-5′), 7.70 (1H, d, $J$ = 9.77 Hz, H-7), 8.41 (1H, d, $J$ = 1.95 Hz, H-10).

**9-Chloro-2-(2-furanyl)-5-[(4-methoxyphenylacetyl)-amino][1,2,4]triazolo[1,5-*c*]quinazoline (4):** $^1$H NMR (DMSO-$d_6$) $\delta$ 3.74 (3H, s, $-OCH_3$), 3.98 (2H, s, $-CH_2CO$), 6.78−6.80 (1H, m, H-4′), 6.93 (2H, d, $J$ = 8.7 Hz, aromatic-H), 7.32−7.35 (3H, m, H-3′ and aromatic-H), 7.92 (2H, s, H-8 and H-7), 8.03 (1H, s, H-5′), 8.39 (1H, s, H-10), 11.24 (1H, s, NH).

**9-Chloro-2-(2-furanyl)-5-[(4-amino-3-iodophenylacetyl)-amino][1,2,4]triazolo[1,5-*c*]quinazoline (5).** To a solution of **6** (10 mg, 0.024 mmol) in 1 mL of $CH_2Cl_2$/MeOH was added solid $I_2$ (6 mg, 0.024 mmol) followed by solid $CaCO_3$ (3 mg, 0.028 mmol). The reaction mixture was stirred for 12 h at room temperature. The solution was evaporated with a nitrogen stream and partitioned between $NaHSO_3$/EtOAc. EtOAc layer was dried over anhydrous $Na_2SO_4$ and evaporated to dryness under reduced pressure. The residue was purified by preparative silica gel TLC ($CHCl_3$−MeOH, 30:1) to afford 3.3 mg of **5** as a brown solid (25%):

$^1$H NMR ($CDCl_3$) $\delta$ 4.13 ($NH_2$, s), 4.22 (2H, s, $-CH_2CO$), 6.63−6.64 (1H, m, H-4′), 6.76 (1H, d, $J$ = 7.9 Hz, aromatic-H), 7.20 (1H, d, $J$ = 7.9 Hz, aromatic-H), 7.28−7.29 (2H, m, H-3′ and aromatic-H), 7.69 (1H, s, H-5′), 7.75 (1H, dd, $J$ = 8.7, 2.9 Hz, H-8), 7.94 (1H, d, $J$ = 8.7 Hz, H-7), 8.50 (1H, d, $J$ = 2.9 Hz, H-10), 9.08 (1H, s, NH).

**9-Chloro-2-(2-furanyl)-5-[(4-aminophenylacetyl)amino]-[1,2,4]triazolo[1,5-*c*]quinazoline (6).** A mixture of $PtO_2$ (5 mg) and 9-chloro-2-(2-furanyl)-5-[(4-nitrophenylacetyl)amino]-[1,2,4]triazolo[1,5-*c*]quinazoline (10 mg, 0.022 mmol), which was prepared using method A, in 3 mL of $CH_2Cl_2$/MeOH, was stirred under hydrogen atmosphere for 3 h at room temperature. The reaction mixture was filtered through a Celite bed, and the filtrate was concentrated and purified by preparative silica gel TLC (Hex:$CHCl_3$:MeOH, 1:1:0.1) to afford 4.1 mg of **6** as a brown solid (45%): $^1$H NMR ($CDCl_3$) $\delta$ 3.74 ($NH_2$, s), 4.16 (2H, s, $-CH_2CO$), 6.61−6.62 (1H, m, H-4′), 6.73 (2H, d, $J$ = 7.8 Hz, aromatic-H), 7.21 (2H, d, $J$ = 7.8 Hz, aromatic-H), 7.24 (1H, m, H-3′), 7.66 (1H, s, H-5′), 7.72 (1H, dd, $J$ = 8.8, 2.9 Hz, H-8), 7.92 (1H, d, $J$ = 8.8 Hz, H-7), 8.45 (1H, d, $J$ = 2.9 Hz, H-10), 9.11 (1H, bs, NH).

**9-Chloro-2-(2-furanyl)-5-[(2-iodophenylacetyl)amino]-[1,2,4]triazolo[1,5-*c*]quinazoline (7):** $^1$H NMR ($CDCl_3$) $\delta$ 4.56 (2H, s, $-CH_2CO$), 6.64−6.65 (1H, m, H-4′), 7.03−7.09 (1H, m, aromatic-H), 7.29 (1H, m, H-3′), 7.41−7.43 (2H, m, aromatic-H), 7.69 (1H, s, H-5′), 7.75 (1H, dd, $J$ = 8.8, 2.9 Hz, H-8), 7.92−7.96 (2H, m, aromatic-H and H-7), 8.51 (1H, d, $J$ = 2.9 Hz, H-10), 9.19 (1H, bs, NH).

**9-Chloro-2-(2-furanyl)-5-[(3-iodophenylacetyl)amino]-[1,2,4]triazolo[1,5-*c*]quinazoline (8):** $^1$H NMR ($CDCl_3$) $\delta$ 4.38 (2H, s, $-CH_2CO$), 6.63−6.65 (1H, m, H-4′), 7.10−7.19 (1H, m, aromatic-H), 7.30−7.31 (1H, m, H-3′), 7.40 (1H, d, $J$ = 7.8 Hz, aromatic-H), 7.64 (1H, d, $J$ = 7.8 Hz, aromatic-H), 7.69 (1H, s, H-5′), 7.75 (1H, dd, $J$ = 8.8, 1.9 Hz, H-8), 7.82 (1H, s, aromatic-H), 7.91 (1H, d, $J$ = 8.8 Hz, H-7), 8.50 (1H, d, $J$ = 1.9 Hz, H-10), 9.10 (1H, bs, NH).

**9-Chloro-2-(2-furanyl)-5-[(4-iodophenylacetyl)amino]-**

**[1,2,4]triazolo[1,5-*c*]quinazoline (9):** $^1$H NMR ($CDCl_3$) $\delta$ 4.37 (2H, s, $-CH_2CO$), 6.64 (1H, s, H-4′), 7.17 (2H, d, $J$ = 7.8 Hz, aromatic-H), 7.28−7.29 (1H, m, H-3′), 7.69−7.76 (4H, m, H-5′, H8 and aromatic-H), 7.90 (1H, d, $J$ = 8.8 Hz, H7), 8.03 (1H, s, H-5′), 8.50 (1H, s, H-10), 9.08 (1H, s, NH).

**9-Chloro-2-(2-furanyl)-5-[(3-chlorophenylacetyl)amino]-[1,2,4]triazolo[1,5-*c*]quinazoline (10):** $^1$H NMR ($CDCl_3$) $\delta$ 4.42 (2H, s, $-CH_2CO$), 6.64−6.65 (1H, m, H-4′), 7.28−7.32 (4H, m, aromatic-H and H-3′), 7.45 (1H, s, aromatic-H), 7.68 (1H, s, H-5′), 7.76 (1H, dd, $J$ = 8.8, 2.9 Hz, H-8), 7.91 (1H, d, $J$ = 8.8 Hz, H-7), 8.50 (1H, d, $J$ = 2.9 Hz, H-10), 9.10 (1H, bs, NH).

**9-Chloro-2-(2-furanyl)-5-[[(2*R*)-phenylpropionyl]amino]-[1,2,4]triazolo[1,5-*c*]quinazoline (11):** $^1$H NMR ($CDCl_3$) $\delta$ 1.69 (3H, d, $J$ = 6.8 Hz, $-CH_3$), 4.54 (1H, q, $J$ = 6.8 Hz, −CHCO), 6.60−6.62 (1H, m, H-4′), 7.20−7.21 (1H, m, H-3′), 7.29−7.50 (5H, m, aromatic-H), 7.65 (1H, s, H-5′), 7.72 (1H, dd, $J$ = 8.8, 2.9 Hz, H-8), 7.94 (1H, d, $J$ = 8.8 Hz, H-7), 8.44 (1H, d, $J$ = 2.9 Hz, H-10), 9.03 (1H, bs, NH); $[\alpha]_D^{20}$ = +1.04 ($c$ = 0.23, $CHCl_3$).

**9-Chloro-2-(2-furanyl)-5-[[(2*S*)-phenylpropionyl]amino]-[1,2,4]triazolo[1,5-*c*]quinazoline (12):** $^1$H NMR ($CDCl_3$) identical to **11**, $[\alpha]_D^{20}$ = −2.26 ($c$ = 0.38, $CHCl_3$).

**9-Chloro-2-(2-furanyl)-5-(diphenylacetylamino)[1,2,4]-triazolo[1,5-*c*]quinazoline (13):** $^1$H NMR ($CDCl_3$) $\delta$ 6.09 (1H, s, −CHCO), 6.61−6.64 (1H, m, H-4′), 7.05−7.45 (11H, m, H-3′ and aromatic-H), 7.65 (1H, s, H-5′), 7.73 (1H, dd, $J$ = 8.8, 2.9 Hz, H-8), 7.92 (1H, d, $J$ = 8.8 Hz, H-7), 8.46 (1H, d, $J$ = 2.9 Hz, H-10), 9.26 (1H, bs, NH).

**9-Chloro-2-(2-furanyl)-5-[(2,2-diphenylpropionyl)amino]-[1,2,4]triazolo[1,5-*c*]quinazoline (14):** $^1$H NMR ($CDCl_3$) $\delta$ 2.18 (3H, s, $-CH_3$), 6.57−6.59 (1H, m, H-4′), 7.06 (1H, d, $J$ = 3.9 Hz, H-3′), 7.29−7.46 (10H, m, aromatic-H), 7.63 (1H, s, H-5′), 7.71 (1H, dd, $J$ = 8.8, 1.9 Hz, H-8), 8.01 (1H, d, $J$ = 8.8 Hz, H-7), 8.45 (1H, d, $J$ = 1.9 Hz, H-10), 9.33 (1H, bs, NH).

**9-Chloro-2-(2-furanyl)-5-[(3-phenylpropionyl)amino]-[1,2,4]triazolo[1,5-*c*]quinazoline (15):** $^1$H NMR ($CDCl_3$) $\delta$ 3.16 (2H, t, $J$ = 7.8 Hz, $-CH_2$), 3.43 (2H, t, $J$ = 7.8 Hz, $-CH_2$), 6.64 (1H, s, H-4′), 7.22−7.25 (1H, m, H-3′), 7.30−7.33 (5H, m, aromatic-H), 7.70 (1H, s, H-5′), 7.74 (1H, dd, $J$ = 8.8, 1.9 Hz, H-8), 7.85 (1H, d, $J$ = 8.8 Hz, H-7), 8.49 (1H, d, $J$ = 1.9 Hz, H-10), 8.98 (1H, bs, NH).

**9-Chloro-2-(2-furanyl)-5-(cinnamoylamino)[1,2,4]triazolo[1,5-*c*]quinazoline (16):** $^1$H NMR ($CDCl_3$) $\delta$ 6.66 (1H, m, H-4′), 7.35 (1H, d, $J$ = 3.9 Hz, H-3′), 7.48−7.49 (3H, m, aromatic-H), 7.68−7.72 (3H, m, H-5′ and aromatic-H), 7.75−7.78 (2H, m, H-8 and olefinic-H), 7.97 (1H, d, $J$ = 8.7 Hz, H-7), 8.02 (1H, d, $J$ = 16.6 Hz, olefinic-H), 8.53 (1H, d, $J$ = 1.9 Hz, H-10), 9.10 (1H, bs, NH).

**5-[[*N*-(*tert*-Butoxycarbonyl)-D-alanyl]amino]-9-chloro-2-(2-furanyl)[1,2,4]triazolo[1,5-*c*]quinazoline (17) and the corresponding L-enantiomer (18):** $^1$H NMR ($CDCl_3$) $\delta$ 1.50 (9H, s, −Boc), 1.58 (3H, d, $J$ = 5.8 Hz, $-CH_3$), 4.95 (1H, m, H-α), 5.13 (1H, bs, NH), 6.64 (1H, m, H-4′), 7.31 (1H, d, $J$ = 2.9 Hz, H-3′), 7.67 (1H, s, H-5′), 7.75 (2H, dd, $J$ = 8.7, 1.9 Hz, H-8), 7.97 (1H, d, $J$ = 8.7 Hz, H-7), 8.51 (1H, d, $J$ = 1.9 Hz, H-10), 9.92 (1H, bs, NH).

**5-[[3-[(*tert*-Butoxycarbonyl)amino]propionyl]amino]-9-chloro-2-(2-furanyl)[1,2,4]triazolo[1,5-*c*]quinazoline (19):** $^1$H NMR ($CDCl_3$) $\delta$ 1.44 (9H, s, −Boc), 3.32 (2H, t, $J$ = 5.8 Hz, $-CH_2$), 3.62 (2H, q, $J$ = 5.8 Hz, $-CH_2$), 5.28 (1H, bs, NH), 6.64 (1H, m, H-4′), 7.31 (1H, d, $J$ = 3.8 Hz, H-3′), 7.68 (1H, s, H-5′), 7.73 (2H, dd, $J$ = 8.8, 1.9 Hz, H-8), 7.87 (1H, d, $J$ = 8.8 Hz, H-7), 8.47 (1H, d, $J$ = 1.9 Hz, H-10), 9.06 (1H, bs, NH).

**5-[[5-[(*tert*-Butoxycarbonyl)amino]pentanoyl]amino]-9-chloro-2-(2-furanyl)[1,2,4]triazolo[1,5-*c*]quinazoline (21):** $^1$H NMR ($CDCl_3$) $\delta$ 1.44 (9H, s, −Boc), 1.63−1.73 (2H, m, $-CH_2$), 1.81−1.92 (2H, m, $-CH_2$), 3.10 (2H, t, $J$ = 6.8 Hz, $-CH_2$), 3.22 (2H, q, $J$ = 6.8 Hz, $-CH_2$), 4.67 (1H, bs, NH), 6.63 (1H, m, H-4′), 7.30 (1H, d, $J$ = 3.9 Hz, H-3′), 7.68 (1H, s, H-5′), 7.72 (2H, dd, $J$ = 8.8, 1.9 Hz, H-8), 7.87 (1H, d, $J$ = 8.8 Hz, H-7), 8.46 (1H, d, $J$ = 1.9 Hz, H-10), 9.01 (1H, bs, NH).

**5-[[6-[(*tert*-Butoxycarbonyl)amino]hexanoyl]amino]-9-chloro-2-(2-furanyl)[1,2,4]triazolo[1,5-*c*]quinazoline (22):** $^1$H NMR ($CDCl_3$) $\delta$ 1.45 (9H, s, −Boc), 1.50−1.61 (4H, m, 2 × $-CH_2$), 1.80−1.90 (2H, m, $-CH_2$), 3.05 (2H, t, $J$ = 6.8 Hz, $-CH_2$), 3.14−3.18 (2H, m, $-CH_2$), 4.66 (1H, bs, NH), 6.62 (1H, m, H-4′), 7.29 (1H, m, H-3′), 7.67 (1H, s, H-5′), 7.70 (2H, dd, $J$ = 8.8, 1.9 Hz, H-8), 7.84 (1H, d, $J$ = 8.8 Hz, H-7), 8.42 (1H, d, $J$ = 1.9 Hz, H-10), 9.01 (1H, bs, NH).

**5-[[7-[(*tert*-Butoxycarbonyl)amino]heptanoyl]amino]-9-chloro-2-(2-furanyl)[1,2,4]triazolo[1,5-*c*]quinazoline (23):** $^1$H NMR ($CDCl_3$) $\delta$ 1.45 (9H, s, −Boc), 1.50−1.61 (6H, m, 3 × $-CH_2$), 1.86 (2H, m, $J$ = 6.85 Hz, $-CH_2$), 3.03 (2H, t, $J$ = 7.81 Hz, $-CH_2$), 3.13 (2H, m, $-CH_2$), 4.59 (1H, bs, NH), 6.63 (1H, m, $J$ = 1.94 Hz, H-4′), 7.30 (1H, s, H-3′), 7.67 (1H, s, H-5′), 7.72 (1H, m, H-8), 7.86 (1H, d, $J$ = 8.79 Hz, H-7), 8.45 (1H, d, $J$ = 2.94 Hz, H-10), 9.01 (1H, s, NH).

**5-[(D-Alanyl)amino]-9-chloro-2-(2-furanyl)[1,2,4]triazolo-[1,5-*c*]quinazoline (24):** $^1$H NMR (DMSO-$d_6$) $\delta$ 1.14 (3H, m, $-CH_3$), 4.25 (1H, bs, H-α), 5.26 (2H, bs, $NH_2$), 6.73 (1H, m, H-4′), 7.12 (1H, m, H-3′), 7.64 (2H, m, H-8 and H-7), 7.93 (1H, m, H-5′), 8.17 (1H, m, H-10), 11.63 (1H, bs, NH); $[\alpha]_D^{20}$ = +6.00 ($c$ = 0.1, $CHCl_3$/$CH_3OH$, 10:1). HPLC retention time: 4.11 min (>95% purity) using solvent system A, 3.91 min (>95% purity) using solvent system B.

**5-[(L-Alanyl)amino]-9-chloro-2-(2-furanyl)[1,2,4]triazolo-[1,5-*c*]quinazoline (25):** $[\alpha]_D^{20}$ = −7.33 ($c$ = 0.09, $CHCl_3$/$CH_3OH$, 10:1). HPLC retention time: 4.09 min (>95% purity) using solvent system A, 4.13 min (>95% purity) using solvent system B.

**5-[(3-Aminopropionyl)amino]-9-chloro-2-(2-furanyl)-[1,2,4]triazolo[1,5-*c*]quinazoline (26):** $^1$H NMR (DMSO-$d_6$) $\delta$ 3.13−3.15 (4H, m, 2 × $-CH_2$), 6.80−6.81 (1H, m, H-4′), 7.36 (1H, d, $J$ = 2.9 Hz, H-3′), 7.83 (2H, bs, $NH_2$), 7.90 (1H, d, $J$ = 8.8 Hz, H-7), 7.95 (1H, dd, $J$ = 8.8, 1.9 Hz, H-8), 8.03 (1H, s, H-5′), 8.42 (1H, d, $J$ = 1.9 Hz, H-10), 11.10 (1H, s, NH).

**5-[(5-Aminopentanoyl)amino]-9-chloro-2-(2-furanyl)-[1,2,4]triazolo[1,5-*c*]quinazoline (28):** $^1$H NMR (DMSO-$d_6$) $\delta$ 1.68 (4H, bs, 2 × $-CH_2$), 2.73−2.76 (2H, m, $-CH_2$), 2.85 (2H, bs, $-CH_2$), 6.78−6.79 (1H, m, H-4′), 7.35 (1H, d, $J$ = 2.9 Hz, H-3′), 7.70 (2H, bs, $NH_2$), 7.92 (2H, s, H-8 and H-7), 8.02 (1H, s, H-5′), 8.40 (1H, s, H-10), 11.07 (1H, s, NH). HPLC retention time: 6.3 min (>95% purity) using solvent system A, 8.7 min (>95% purity) using solvent system B.

**5-[(6-Aminohexanoyl)amino]-9-chloro-2-(2-furanyl)-[1,2,4]triazolo[1,5-*c*]quinazoline (29):** $^1$H NMR (DMSO-$d_6$) $\delta$ 1.42−1.70 (6H, m, 3 × $-CH_2$), 2.72 (2H, t, $J$ = 6.8 Hz, $-CH_2$), 2.81 (2H, t, $J$ = 6.8 Hz, $-CH_2$), 6.78−6.79 (1H, m, H-4′), 7.34 (1H, d, $J$ = 3.9, H-3′), 7.70 (2H, bs, $NH_2$), 7.92 (2H, d, $J$ = 1.9 Hz, H-8 and H-7), 8.01 (1H, s, H-5′), 8.40 (1H, s, H-10), 11.04 (1H, s, NH).

**5-[(7-Aminoheptanoyl)amino]-9-chloro-2-(2-furanyl)-[1,2,4]triazolo[1,5-*c*]quinazoline (30):** $^1$H NMR (DMSO-$d_6$) $\delta$ 1.24 (2H, m, $-CH_2$), 1.39 (2H, m, $-CH_2$), 1.53 (2H, m, $-CH_2$), 1.66 (2H, m, $-CH_2$), 2.71 (2H, m, $-CH_2$), 2.78 (2H, m, $-CH_2$), 6.79 (1H, s, H-4′), 7.35 (1H, s, H-3′), 7.64 (2H, bs, $NH_2$), 7.93 (2H, s, H-7 and H-8), 8.02 (1H, s, H-5′), 8.40 (1H, s, H-10), 11.04 (1H, s, NH). HPLC retention time: 4.6 min (>95% purity) using solvent system A, 8.5 min (>95% purity) using solvent system B.

**5-[[5-(Benzyloxycarbonyl)pentanoyl]amino]-9-chloro-2-(2-furanyl)[1,2,4]triazolo[1,5-*c*]quinazoline (31).** The title compound was synthesized using method B with monobenzyl adipate, which was prepared according to the literature:[39] $^1$H NMR ($CDCl_3$) $\delta$ 1.82−1.88 (4H, m, 3 × $-CH_2$), 2.48 (2H, t, $J$ = 6.8 Hz, $-CH_2$), 3.09 (2H, t, $J$ = 6.8 Hz, $-CH_2$), 5.13 (2H, s, $-CH_2$), 6.62−6.63 (1H, m, H-4′), 7.28−7.36 (6H, m, H-3′ and aromatic-H), 7.67−7.72 (2H, m, H-8 and H-5′), 7.84 (1H, d, $J$ = 8.8 Hz, H-7), 8.44 (1H, d, $J$ = 1.9 Hz, H-10), 8.97 (1H, s, NH).

**5-[[3-(Methoxycarbonyl)propionyl]amino]-9-chloro-2-(2-furanyl)[1,2,4]triazolo[1,5-*c*]quinazoline (32):** $^1$H NMR ($CDCl_3$) $\delta$ 2.86 (2H, t, $J$ = 6.8 Hz, $-CH_2$), 3.44 (2H, t, $J$ = 6.8 Hz, $-CH_2$), 3.75 (3H, s, $-OCH_3$), 6.62−6.64 (1H, m, H-4′), 7.28−7.31 (1H, m, H-3′), 7.68 (1H, s, H-5′), 7.72 (1H, d, $J$ = 8.8, 1.9 Hz, H-8), 7.86 (1H, d, $J$ = 8.8 Hz, H-7), 8.46 (1H, d, $J$ = 1.9 Hz, H-10), 9.12 (1H, s, NH).

**5-[[7-(Methoxycarbonyl)heptanoyl]amino]-9-chloro-2-**

**(2-furanyl)[1,2,4]triazolo[1,5-*c*]quinazoline (33):** $^1$H NMR ($CDCl_3$) $\delta$ 1.47 (2H, m, $-CH_2$), 1.68 (2H, t, $J$ = 6.83 Hz, $-CH_2$), 1.85 (2H, t, $J$ = 6.83 Hz, $-CH_2$), 2.34 (2H, t, $J$ = 7.81 Hz, $-CH_2$), 3.05 (2H, t, $J$ = 7.81 Hz, $-CH_2$), 3.67 (3H, s, $-OCH_3$), 6.65 (1H, s, H-4′), 7.33 (1H, d, $J$ = 3.91 Hz, H-3′), 7.69 (1H, s, H-5′), 7.76 (1H, d, $J$ = 6.84 Hz, H-8), 7.89 (1H, d, $J$ = 9.96 Hz, H-7), 8.50 (1H, d, $J$ = 1.95 Hz, H-10), 8.99 (1H, s, NH).

**5-[(4-Carboxylbutanoyl)amino]-9-chloro-2-(2-furanyl)-[1,2,4]triazolo[1,5-*c*]quinazoline (34).**

A solution of 30 mg (0.105 mmol) of **1a** and 60 mg (0.525 mmol) of glutaric anhydride in 2 mL of acetone was refluxed at 85 °C for 2 days. After cooling, the mixture was purified by preparative silica gel TLC ($CHCl_3$:MeOH, 10:1) and crystallization from $CH_2Cl_2$ to afford 23 mg of **34** as a white solid: $^1$H NMR (DMSO-$d_6$) $\delta$ 1.87 (2H, t, $J$ = 6.8 Hz, $-CH_2$), 2.35 (2H, t, $J$ = 6.8 Hz, $-CH_2$), 2.73 (2H, t, $J$ = 6.8 Hz, $-CH_2$), 6.77 (1H, s, H-4′), 7.33 (1H, s, H-3′), 7.89 (2H, s, H-7 and H-8), 8.00 (1H, s, H-5′), 8.37 (1H, s, H-10).

**Pharmacology. Radioligand Binding Studies.** Binding of [$^3$H]-(*R*)-$N^6$-(phenylisopropyl)adenosine ([$^3$H]*R*-PIA; Amersham, Chicago, IL) to $A_1$ receptors from rat cerebral cortical membranes and of [$^3$H]CGS 21680 (DuPont NEN, Boston, MA) to $A_{2A}$ receptors from rat striatal membranes was performed as described previously.[4,5] Adenosine deaminase (3 units/mL) was present during the preparation of the brain membranes, in a preincubation of 30 min at 30 °C, and during the incubation with the radioligands.

Binding of [$^{125}$I]-$N^6$-(4-amino-3-iodobenzyl)-5′-(*N*-methylcarbamoyl)adenosine ([$^{125}$I]AB-MECA; Amersham) in membranes prepared from HEK-293 cells stably expressing the human $A_3$ receptor (Receptor Biology, Inc., Baltimore, MD) was as described.[24] The assay medium consisted of a buffer containing 50 mM Tris, 10 mM $Mg^{2+}$, and 1 mM EDTA, at pH 8.0. The glass incubation tubes contained 100 $\mu$L of the membrane suspension (0.3 mg of protein/mL, stored at −80 °C in the same buffer), 50 $\mu$L of [$^{125}$I]AB-MECA (final concentration 0.3 nM), and 50 $\mu$L of a solution of the proposed antagonist. Nonspecific binding was determined in the presence of 200 $\mu$M NECA.

All nonradioactive compounds were initially dissolved in DMSO and diluted with buffer to the final concentration, where the amount of DMSO never exceeded 2%.

Incubations were terminated by rapid filtration over Whatman GF/B filters, using a Brandell cell harvester (Brandell, Gaithersburg, MD). The tubes were rinsed three times with 3 mL of buffer each.

At least five different concentrations of competitor, spanning 3 orders of magnitude adjusted appropriately for the $IC_{50}$ of each compound, were used. $IC_{50}$ values, calculated with the nonlinear regression method implemented in the InPlot program (Graph-PAD, San Diego, CA), were converted to apparent $K_i$ values using the Cheng−Prusoff equation[40] and $K_d$ values of 1.0 nM ([$^3$H]*R*-PIA), 14 nM ([$^3$H]CGS 21680), and 0.59 nM ([$^{125}$I]AB-MECA at human $A_3$ receptors). Hill coefficients of the tested compounds were in the range of 0.8−1.1.

**Cyclic AMP Assay of Antagonist Potency at the Human $A_{2B}$ Receptor: 1. Cell Culture.** CHO-$A_{2B}$ cells were grown under 5% $CO_2$/95% $O_2$ humidified atmosphere at a temperature of 37 °C in DMEM supplemented with Hams F12 nutrient mixture (1/1), 10% newborn calf serum, 2 mM glutamine, and containing 50 IU/mL penicillin, 50 $\mu$g/mL streptomycin, and 0.2 mg/mL Geneticin (G418, Boehringer Mannheim). Cells were cultured in 10-cm diameter round plates and subcultured when grown confluent (approximately after 72 h). PBS/EDTA containing 0.25% trypsin was used for detaching the cells from the plates. Experimental cultures were grown overnight as a monolayer in 24-well tissue culture plates (400 $\mu$L/well; $0.8 \times 10^6$ cells/well). CHO-$A_{2B}$ cells were kindly provided by Dr. K.-N. Klotz (University of Würzburg, Germany).

**2. Cyclic AMP Generation.** Cyclic AMP generation was performed in DMEM/HEPES buffer (DMEM containing 50 mM HEPES, pH 7.4, 37 °C). To each well, washed twice with DMEM/HEPES buffer, were added 100 $\mu$L of adenosine deaminase (final concentration 10 IU/mL) and 100 $\mu$L of rolipram/cilostamide (final concentration 10 $\mu$M/10 $\mu$M), followed by 50 $\mu$L of test compound (appropriate concentration) or buffer. After incubation for 40 min at 37 °C, 100 $\mu$L of NECA was added (final concentration 50 $\mu$M for compound screening and $IC_{50}$ determination, appropriate concentrations for recording dose−response curves for p$A_2$ calculations). After 15 min, incubation at 37 °C was terminated by removing the medium and adding 200 $\mu$L of 0.1 M HCl. Wells were stored at −20 °C until assay.

**3. Cyclic AMP Determination.** The amounts of cyclic AMP were determined after a protocol with cAMP binding protein (PKA)[41] with the following minor modifications. As a buffer was used 150 mM $K_2HPO_4$/10 mM EDTA/0.2% BSA FV at pH 7.5. Samples (20 $\mu$L) were incubated for 90 min at 0 °C. Incubates were filtered over GF/C glass microfiber filters in a Brandel M-24 cell harvester. The filters were additionally rinsed with 4 × 2 mL of 150 mM $K_2HPO_4$/10 mM EDTA (pH 7.5, 4 °C). Punched filters were counted in Packard emulsifier safe scintillation fluid after 2 h of extraction.

**Abbreviations:** AcOH, acetic acid; Boc, *tert*-butoxycarbonyl; CGS 21680, 2-[[4-(2-carboxyethyl)phenyl]ethylamino]-5′-(*N*-ethylcarbamoyl)adenosine; CGS 15943, 9-chloro-2-(2-furanyl)-[1,2,4]triazolo[1,5-*c*]quinazolin-5-amine; CHO cells, Chinese hamster ovary cells; DMAP, 4-(dimethylamino)pyridine; EDAC, 3-ethyl-1-(3-(dimethylamino)propyl)carbodiimide; DMF, *N*,*N*-dimethylformamide; DMSO, dimethyl sulfoxide; EDTA, ethylenediaminetetraacetate; EI, electric ionization; CI, chemical ionization; FAB, fast atom bombardment; HEK cells, human embryonic kidney cells; HMPA, hexamethylphosphotriamide; [$^{125}$I]AB-MECA, [$^{125}$I]-$N^6$-(4-amino-3-iodobenzyl)adenosine-5′-*N*-methyluronamide; $K_i$, equilibrium inhibition constant; MS, mass spectrum; NECA, 5′-(*N*-ethylcarbamoyl)adenosine; *R*-PIA, (*R*)-$N^6$-(phenylisopropyl)adenosine; SAR, structure−activity relationship; TFA, trifluoroacetic acid; THF, tetrahydrofuran; TLC, thin-layer chromatography; Tris, tris(hydroxymethyl)aminomethane; TEAA, triethylammonium acetate.

## References


(1) Müller, C. E. $A_1$-adenosine receptor antagonists. *Exp. Opin. Ther. Patents* **1997**, *7*, 419−440.

(2) Baraldi, P. G.; Cacciari, B.; Spalluto, G.; Borioni, A.; Viziano, M.; Dionisotti, S.; Ongini, E. Current developments of $A_{2A}$ adenosine receptor antagonists. *Curr. Med. Chem.* **1995**, *2*, 707−722.

(3) Müller, C. E.; Stein, B. Adenosine receptor antagonists − structures and potential therapeutic applications. *Curr. Pharm. Des.* **1996**, *2*, 501−530.

(4) Schwabe, U.; Trost, T. Characterization of adenosine receptors in rat brain by (−) [$^3$H]$N^6$-phenylisopropyladenosine. *Naunyn-Schmiedeberg's Arch. Pharmacol.* **1980**, *313*, 179−187.

(5) Jarvis, M. F.; Schutz, R.; Hutchison, A. J.; Do, E.; Sills, M. A.; Williams, M. [$^3$H]CGS 21680, an $A_2$ selective adenosine receptor agonist directly labels $A_2$ receptors in rat brain tissue. *J. Pharmacol. Exp. Ther.* **1989**, *251*, 888−893.

(6) Fredholm, B. B. Adenosine and neuroprotection. *Intl. Rev. Neurobiol.* **1997**, *40*, 259−280.

(7) Ongini, E.; Dionisotti, S.; Morelli, M.; Ferre, S.; Svenningsson, P.; Fuxe, K.; Fredholm, B. B. Neuropharmacology of the adenosine A2A receptors. *Drug Dev. Res.* **1996**, *39*, 450−460.

(8) Latini, S.; Pazzagli, M.; Pepeu, G.; Pedata, F. $A_2$ adenosine receptors − their presence and neuromodulatory role in the central-nervous-system. *Gen. Pharmacol.* **1996**, *27*, 925−933.

(9) Mehra, A.; Cohen, G.; Johnson, J. V.; Elkayam, U. Effect of adenosine on the renal circulation in patients with chronic heart-failure. *J. Am. Coll. Cardiol.* **1997**, *29*, 7834−7834.

(10) Rongen, G. A.; Floras, J. S.; Lenders, J.; Thien, T.; Smits, P. Cardiovascular pharmacology of purines. *Clin. Sci.* **1997**, *92*, 13−24.

(11) Jacobson, K. A.; Suzuki, F. Recent developments in selective agonists and antagonists acting at purine and pyrimidine receptors. *Drug Dev. Res.* **1996**, *39*, 289−300.

(12) Jacobson, K. A.; von Lubitz, D. K. J. E.; Daly, J. W.; Fredholm, B. B. Adenosine receptor ligands − differences with acute versus chronic treatment. *Trends Pharmacol. Sci.* **1996**, *17*, 108−113.

(13) Tracey, W. R.; Magee, W.; Masamune, H.; Kennedy, S. P.; Knight, D. R.; Buchholz, R. A.; Hill, R. J. Selective adenosine $A_3$ receptor stimulation reduces ischemic myocardial injury in the rabbit heart. *Cardiovasc. Res.* **1997**, *33*, 410−415.

(14) Kohno, Y.; Sei, Y.; Koshiba, M.; Kim, H. O.; Jacobson, K. A. Induction of apoptosis in HL-60 human promyelocytic leukemia-cells by adenosine $A_3$ receptor agonists. *Biochem. Biophys. Res. Commun.* **1996**, *221*, 849−849.
(15) Karton, Y.; Jiang, J. L.; Ji, X. D.; Melman, N.; Olah, M. E.; Stiles, G. L.; Jacobson, K. A. Synthesis and biological-activities of flavonoid derivatives as as adenosine receptor antagonists. *J. Med. Chem.* **1996**, *39*, 2293−2301.
(16) Jacobson, M. A.; Chakravarty, P. K.; Johnson, R. G.; Norton, R. Novel nonxanthine selective $A_3$ adenosine receptor antagonists. *Drug. Dev. Res.* **1996**, *37*, 131−131.
(17) van Rhee, A. M.; Jiang, J. L.; Melman, N.; Olah, M. E.; Stiles, G. L.; Jacobson, K. A. Interaction of 1,4-dihydropyridine and pyridine-derivatives with adenosine receptors − selectivity for $A_3$ receptors. *J. Med. Chem.* **1996**, *39*, 2980−2989.
(18) Jiang, J. L.; Van Rhee, A. M.; Melman, N.; Ji, X. D.; Jacobson, K. A. 6-phenyl-1,4-dihydropyridine derivatives as potent and selective $A_3$ adenosine receptor antagonists. *J. Med. Chem.* **1996**, *39*, 4667−4675.
(19) Jiang, J. L.; Van Rhee, A. M.; Chang, L.; Patchornik, A.; Ji, X. D.; Evans, P.; Melman, N.; Jacobson, K. A. Structure−activity-relationships of 4-(phenylethynyl)-6-phenyl-1,4-dihydropyridines as highly selective $A_3$ adenosine receptor antagonists. *J. Med. Chem.* **1997**, *40*, 2596−2608.
(20) Kim, Y. C.; Ji, X. D.; Jacobson, K. A. Derivatives of the triazoloquinazoline adenosine antagonist (CGS15943) are selective for the human $A_3$ receptor subtype. *J. Med. Chem.* **1996**, *39*, 4142−4148.
(21) Jacobson, M. A.; Johnson, R. G.; Luneau, C. J.; Salvatore, C. A. Cloning and chromosomal localization of the human $A_{2B}$ adenosine receptor gene (ADORA2B) and its pseudogene. *Genomics* **1995**, *27*, 374−376.
(22) Gallo-Rodriguez, C.; Ji, X. D.; Melman, N.; Siegman, B. D.; Sanders, L. H.; Orlina, J.; Fischer, B.; Pu, Q. L.; Olah, M. E.; van Galen, P. J. M.; Stiles, G. L.; Jacobson, K. A. Structure−activity-relationships of N-6-benzyladenosine-5′-uronamides as $A_3$-selective adenosine agonists. *J. Med. Chem.* **1994**, *37*, 636−646.
(23) Salvatore, C. A.; Jacobson, M. A.; Taylor, H. E.; Linden, J.; Johnson, R. G. Molecular cloning and characterization of the human $A_3$ adenosine receptor. *Proc. Natl. Acad. Sci. U.S.A.* **1993**, *90*, 10365−10369.
(24) Olah, M. E.; Gallo-Rodriguez, C.; Jacobson, K. A.; Stiles, G. L. [$^{125}$I]AB-MECA, a high affinity radioligand for the rat $A_3$ adenosine receptor. *Mol. Pharmacol.* **1994**, *45*, 978−982.
(25) Kim, J.; Wess, J.; van Rhee, A. M.; Schoneberg, T.; Jacobson, K. A. Site-directed mutagenesis identifies residues involved in ligand recognition in the human $A_{2a}$ adenosine receptor. *J. Biol. Chem.* **1995**, *270*, 13987−13997.
(26) Moro, S.; Guo, D.; Camaioni, E.; Boyer, J. L.; Harden, K.; Jacobson, K. A. Human $P2Y_1$ receptor: molecular modeling and site-directed mutagenesis as a tools to identify agonist and antagonist recognition sites. *J. Med. Chem.* **1998**, *41*, 1456−1466.
(27) Lin, Z.; Shenker, A.; Pearlstein, R. A model of the lutropin/choriogonadotropin receptor: insights into the structural and functional effects of constitutively activating mutations. *Protein Eng.* **1997**, *10*, 501−510.
(28) Chiota, C.; Levitt, M.; Richardson, D. Helix to helix packing in proteins. *J. Mol. Biol.* **1981**, *145*, 215−250.
(29) Schertler, G. F.; Villa, C.; Henderson, R. Projection structure of rhodopsin. *Nature* **1993**, *362*, 770−772.
(30) Urger, V. M.; Hargrave, P. A.; Baldwin, J. M.; Schertler, G. F. X. Arrangement of rhodopsin transmembrane α-helices. *Nature* **1997**, *389*, 203−206.
(31) Gouldson, P. R.; Snell, C. R.; Reynolds, C. A. A new approach to docking in the $\beta_2$-adrenergic receptor that exploits the domain structure of G-protein-coupled receptors. *J. Med. Chem.* **1997**, *40*, 3871−3886.
(32) Olah, M. E.; Ren, H. Z.; Ostrowski, J.; Jacobson, K. A.; Stiles, G. L. Cloning, expression, and characterization of the unique bovine $A_1$ adenosine receptor. Studies on the ligand binding site by site-directed mutagenesis. *J. Biol. Chem.* **1992**, *267*, 10764−10770.
(33) Kim, J.; Jiang, Q.; Glashofer, M.; Yehle, S.; Wess, J.; Jacobson, K. A. Glutamate residues in the second extracellular loop of the human $A_{2a}$ adenosine receptor are required for ligand recognition. *Mol. Pharmacol.* **1996**, *49*, 683−691.
(34) The program SYBYL 6.3 is available from TRIPOS Associates, St. Louis, MO; 1993.
(35) Mohamadi, F.; Richards, N. G. J.; Guida, W. C.; Liskamp, R.; Lipton, M.; Caufield, C.; Chang, G.; Hendrickson, T.; Still, W. C. MacroModel-An Integrated Software System for Modeling Organic and Bioorganic Molecules using Molecular Mechanics. *J. Comput. Chem.* **1990**, *11*, 440−450.
(36) van Rhee, A. M.; Fischer, B.; van Galen, P. J. M.; Jacobson, K. A. Modeling the $P_{2Y}$ purinoceptor using rhodopsin as template. *Drug Des. Discov.* **1995**, *13*, 133−154.
(37) Kyte, J.; Doolittle, R. F. A simple method for displaying the hydrophobic character of a protein. *J. Mol. Biol.* **1982**, *157*, 105−132.
(38) Weiner, S. J.; Kollman, P. A.; Nguyen, D. T.; Case, D. A. An all-atom force field for simulation of protein and nucleic acids. *J. Comput. Chem.* **1986**, *7*, 230−252.
(39) English, A. R.; Girard, D.; Jasys, V. J.; Martingano, R. J.; Kellogg, M. S. Orally Effective Acid Prodrugs of the $\beta$-Lactamase Inhibitor Sulbactam. *J. Med. Chem.* **1990**, *33*, 344−347.
(40) Cheng, Y. C.; Prusoff, W. H. Relationship between the inhibition constant ($K_i$) and the concentration of inhibitor which causes 50% inhibition ($IC_{50}$) of an enzyme reaction. *Biochem. Pharmacol.* **1973**, *22*, 3099−3108.
(41) van der Wenden, E. M.; Hartog-Witte, H. R.; Roelen, H. C. P. F.; von Frijtag Drabbe Künzel, J. K.; Pirovano, I. M.; Mathôt, R. A. A.; Danhof, M.; van Aerschot, A.; Lidaks, M. J.; IJzerman, A. P.; Soudijn, W. 8-Substituted adenosine and theophylline-7-riboside analogues as potential partial agonists for the adenosine $A_1$ receptor. *Eur. J. Pharmacol.-Mol. Pharmacol. Sect.* **1995**, *290*, 189−199.
(42) Alexander, S. P. H.; Cooper, J.; Shine, J.; Hill, S. J. Characterization of the human brain putative A2B adenosine receptor expressed in Chinese hamster ovary (CHO.A2B.4) cells. *Br. J. Pharmacol.* **1996**, *119*, 1286−1290.
(43) Feoktistov, I.; Biaggioni, I. Adenosine $A_{2B}$ receptors. *Pharmacol. Rev.* **1997**, *49*, 381−402.

JM980094B